Leaf Model Reconstruction and Mechanical Deformation Based on Laser Point Cloud

Ting Yun[1], Weizheng Li[2], Yuan Sun[3], Lianfeng Xue[1*]

[1]*Department of Information Science and Technology*
Nanjing Forestry University
159 Longpan Road, Nanjing, Jiangsu, P. R. China
E-mails: njyunting@qq.com, 285201972@qq.com

[2]*Advanced Analysis and Testing Center*
Nanjing Forestry University
159 Longpan Road, Nanjing, Jiangsu, P. R. China
E-mail: gisplayer@gmail.com

[3]*Department of Forest Resource and Environment*
Nanjing Forestry University
159 Longpan Road, Nanjing, Jiangsu, P. R. China
E-mail: sunyuan1123@126.com

[*]*Corresponding author*

Received: May 26, 2014 **Accepted: September 22, 2014**

Published: September 30, 2014

Abstract: *In recent years, terrestrial laser scanning has been widely used in complex scene investigation and space object measurement. However, due to the irregular and complex topology of leaves and also multi-view occlusion and interference caused by external environment, reconstructing real 3D leaf model based on the point cloud data is a challenging task. In this paper, we propose a method for leaf surface reconstruction and deformation under external force. Firstly, the polynomial fitting method is designed to locate the accurate leaf boundaries from scanned point cloud. Moreover leaf midvein and lateral veins are delineated by designed skeleton extraction algorithm. Secondly, in order to get lifelike and smoothing leaf surface and eliminate interference caused by leaf jitter in the wind, the generalized tensor product bicubic Bezier surface method is adopted to fit the foliar point cloud data and construct the real 3D leaf model. Thirdly, according to solid mechanics force theory, leaf surface is divided into two parts of mesophyll and vein with different material properties. Then each part is subdivided by tetrahedron mesh, and new stress deformation equations based on the nonlinear finite element are constructed to simulate leaf deformation under various external force. Finally, verified by experimental results, our method is feasible and reasonable to the broad-leaved tree's leaves, and our methodology and simulation process also provide the great potential for further study on evolutions of flowers and leaves under various environmental conditions.*

Keywords: *Terrestrial laser scanning, Point cloud data, Leaf model reconstruction, Leaf deformation under force.*

Introduction

In the nature, leaves perform three important functions such as manufacture of food, photosynthesis and beautification environment. How to solve and explore the fine measurement of tree leaves and provide an effective way to improve the accuracy and efficiency of leaf analysis is a main task in forestry management.

In recent years, modeling trees and plants has seen quite a lot of attention from the scientific community. Combing with physics and structural mechanics theory, Chi et al. [2] proposed

a botanical and physical method to simulate variations of leaf shape, he converted leaf to a double layered model, which composed by mesophyll cells and vein cells, by setting up the mass-spring system in these interconnecting layers, different kinetic manners of mesophyll and veins can be simulated respectively to present weathering plant leaves. Zhu et al. [10] presented a novel method to deform the tree model interactively using cages based on trees' property and a framework of hierarchy deformation, thus he manipulated the model vertices of tree positions to achieve the deformation. Liu et al. [3] used the inhomogeneous field theory to simulate the swelling- and deswelling-induced instabilities of various membrane structures. Moreover, he designed the finite element subroutine developed in ABAQUS software. His study has been made in attempt to mimic the shape of a plant leaves from the swelling/deswelling patterns of a gel and explore the possible origin of intriguing natural phenomena of plants. Zeng et al. [7] presented a new scheme using functional structural plant model (FSPM) and employing feedback control system (FCS) to realize the multi-scale change of the physiological parameter for leaf growth. In addition, the varying vein texture is synthesized by reaction-diffusion principle based on the canalization hypothesis. At last, the controllability of grid bending is realized to achieve leaf deformation.

Terrestrial laser scanning (TLS), also known as the most advanced measuring instruments, has already been used in practical plant analysis in the developed countries. The TLS scans pulse laser over the full upper hemisphere and part of the lower hemisphere by using a mirror rotating in the vertical plane (the zenith scan) and a rotation of the instrument to provide azimuthal coverage. The time-dependent intensity of reflected light from each laser pulse is recorded, providing a waveform that may include responses from multiple targets [4, 5]. Reflections from targets are time-delayed copies of this pulse where the range to the target is simply inferred from the arrival time of the pulse peak relative to the peak of the outgoing pulse. TLS can mosaic the multi-view scanning data, thereby ensuring scanning data completeness and reducing the impact of foliage cover, and eventually getting the 3D Point Cloud Data (PCD) of real stumpage. Due to high-precision and high-density characteristics, the TLS-based method is taken as a most appropriate method for tree measurement; it can also serve as a calibration tool for airborne laser scanning and other measurement application with ground sampling.

Zheng and Moskal [8] used convex hull algorithm for the projection PCD of the single leaf on the X-Y plane to compute the extinction coefficient in the single voxel, and estimated Effective Leaf Area (ELA) from PCD. Xu et al. [6] presented a semi-automatic method for transforming the sparse point clouds obtained from scanning to polygonal models. A skeleton of the trunk and main branches was produced based on the scanned point clouds. Then steps were taken to synthesize additional branches to produce plausible support for the tree crown. Subsequently, allometric theory was used to estimate appropriate dimensions for each branch. At last, leaves were positioned, oriented and connected to nearby branches. Zheng and Moskal [9] combined beer laws to present a new method that used total least square fitting techniques to reconstruct the normal vectors and then indirectly and nondestructively retrieved foliage elements' orientation and distribution from PCD obtained using TLS approach.

In this paper, we divide leaf into two parts mesophyll and vein, and each part is given with different material properties. Meanwhile a new method combined with computer graphics and physics theory for foliage modeling and force-induced deformation is presented, and the details are shown in the following sections.

Materials and methods

Data collection by terrestrial laser scanner

We use Leica Scan Station C10 to scan michelia tree and sakura tree on the campus and obtain leaves' PCD for calculation. The specifications of C10 are described in Table 1, and Fig. 1 shows our experiment about tree data acquisition using Leica C10 scanner.

Table 1. The specifications of Leica Scan Station C10

Leica Scan Station C10 Technical details	
Accuracy of single measurement [Position/Distance/Angular]	6mm/4mm/60μrad(12")
Range	300 m @ 90%; 134 m @ 18% albedo (minimum range 0.1 m)
Scan resolution Spot size Point spacing	From 0-50 m: 4.5 mm (FWHH-based); 7 mm (Gaussian-based), Fully selectable horizontal and vertical; <1 mm minimum spacing
Laser plummet	Laser class: (IEC 60825-1) Centering accuracy: 1.5 mm Laser dot diameter: 2.5 mm
Laser color	Green, wavelength = 532 nm visible
Environmental lighting	Fully operational between bright sunlight and complete darkness

Fig. 1 Using Leica Scan Station C10 to scan trees on campus

Leaf vein extraction

Due to disturbance caused by external environment and multi-view occlusion, there exist interference and noise among obtained scanning PCD, so how to remove the measurement deviation and design appropriate algorithm to get real foliage model is to be considered. In this section, we design algorithm to extract the leaf vein from PCD and reconstruct the leave surface, the specific steps are as follows:

1) Firstly, we choose both endpoints from whole foliage PCD, which represent both sides of leaf's midvein, shown as blue line in Fig. 2 and recorded as: $p_e = (x_e, y_e, z_e)^{\mathrm{T}}$, $p_s = (x_s, y_s, z_s)^{\mathrm{T}}$, here p_e is the lowest point of midvein, and p_s is top point of the midvein. The connective line L_1 between p_e and p_s is considered as the leaf midvein with the equation form of $p = p_e + t(p_s - p_e)$, and the slope of L_1 is $\vec{k}_1 = (p_s - p_e)$. Consequently, we choose the sampling points $p_{L_1,i}$, $i = 1, 2, ..., n+1$ along the midvein L_1 at regular interval, and combine with normal vector $\vec{k}_2 = -1/(p_s - p_e)$ to construct the leaf lateral veins $L_{2,i}$, $\vec{k}_2$ being orthogonal to the vector $\vec{k}_1 = (p_s - p_e)$. Here $L_{2,i}$ is denoted as $p = p_{L_1,i} + t\vec{k}_2$. According to the two side endpoints of each line $L_{2,i}$, the initial edge points of foliage are obtained, and $n+1$ longitudinal skeleton lines $L_{2,i}$, that is the leaf's lateral veins, are constructed.

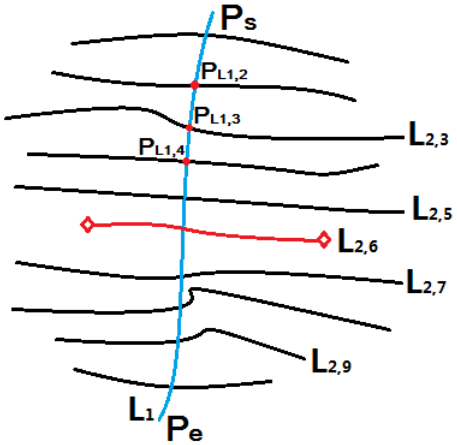

Fig. 2 Selection of leaf skeleton lines

2) For every lateral vein $L_{2,i}$, the endpoints of each $L_{2,i}$ are recorded as $p_{2,li}(x_{l,i}, y_{l,i}, z_{l,i})$ and $p_{2,ri}(x_{r,i}, y_{r,i}, z_{r,i})$, where $i = 1, 2, ..., n$. Due to the noise and occlusion existing in the leaf PCD, the endpoints $(x_{l,i}, y_{l,i}, z_{l,i})$ $(x_{r,i}, y_{r,i}, z_{r,i})$ of each $L_{2,i}$ with deviation values should be abandoned, just as shown in Fig. 2. The endpoint values of $L_{2,6}$ are different from the values of the adjacent lines, so we believe data corruption exists in the line $L_{2,6}$ and should be discarded.

3) Through our algorithm processing, we can get the correct and effective leaf edge points. The left and right endpoints of every lateral veins are respectively denoted as:

$$p_{2,lj} = \{(x_{l,1}, y_{l,1}, z_{l,1}), (x_{l,2}, y_{l,2}, z_{l,2}), ..., (x_{l,j}, y_{l,j}, z_{l,j})\},$$
$$p_{2,rj} = \{(x_{r,1}, y_{r,1}, z_{r,1}), (x_{r,2}, y_{r,2}, z_{r,2}), ..., (x_{r,j}, y_{r,j}, z_{r,j})\}.$$

These edge points also constitute the initial scanning contour of the leaf. For the each side endpoints of lateral veins, we originally propose surface fitting and intersection algorithm to locate the true leaf boundary without a loss of morphological features. The specific sequence

is as follows: For the left (or right) side of the endpoints $p_{2,li}\left(x_{l,i}, y_{l,i}, z_{l,i}\right)$, we take the $\left\{x_{l,i}, y_{l,i}\right\}$, $i = 1, 2, ..., n$ as a group of input foliage geometric edge parameters. Using the polynomial curve fitting method, the magnitudes of y_l are taken as input parameters to calculate the corresponding fitting values of x_l', z_l', so a series of polynomial coefficient is calculated to make the data x_l' fit to x_l, the regression equations are described as follows:

$$x_l \approx x_l' = v_x\left(y_l\right) = v_{x1}y_l^n + v_{x2}y_l^{n-1} + v_{x3}y_l^{n-2} + ... + v_{xn'-1}y_l + v_{xn'},$$
$$z_l \approx z_l' = v_z\left(y_l\right) = v_{z1}y_l^n + v_{z2}y_l^{n-1} + v_{z3}y_l^{n-2} + ... + v_{zn'-1}y_l + v_{zn'}. \quad (1)$$

After transform of our polynomial fitting method, we extract genuine leaf boundary points $p_{edge}' = \left\{x_l', y_l, z_l'; x_r', y_r, z_r'\right\}$ from PCD, so the smooth and real foliage boundary edge is got. In this section for the TLS foliage edge points with non-uniform spatially characteristic, the scientific principle is using the polynomial fitting method to make edge points respectively project onto X-Y plane and Y-Z plane, thus, the two projective surfaces are constructed and the intersection method between the two surfaces is adopted to accurately position the continuous and smooth leaf edge.

Leaf surface reconstruction by bicubic tensor-product Bezier surface

In this section, we used bicubic tensor-product Bezier surface patches to reconstruct foliage surface. For the inner point $p_{i,j}$ of leaf PCD, a tensor-product Bezier surface is defined as:

$$Q(u,v) = \sum_{i=0}^{m}\sum_{j=0}^{n} p_{i,j}B_{i,m}(u)B_{j,n}(v), \quad (2)$$

where j represents which lateral vein $L_{2,j}$ that $p_{i,j}$ belongs to, and i represents the points belong to the lateral vein $L_{2,j}$. $B_{i,m}(u)$ and $B_{j,n}(v)$ are univariate blending functions. The specific form of blending functions is:

$$B_{i,m} = \begin{cases} B_{0,m}(u) = (1-u)^3 \\ B_{1,m}(u) = 3u(1-u)^2 \\ B_{2,m}(u) = 3u^2(1-u) \\ B_{3,m}(u) = (u)^3 \end{cases}, \; B_{j,n} = \begin{cases} B_{0,n}(v) = (1-v)^3 \\ B_{1,n}(v) = 3v(1-v)^2 \\ B_{2,n}(v) = 3v^2(1-v) \\ B_{3,n}(v) = (v)^3 \end{cases}. \quad (3)$$

The equation of our tensor-product Bezier surface is:

$$Q\left(U, V\right) = \sum_{i=0}^{m}\sum_{j=0}^{n}[p_{i,j} + \left(U - \overline{x}_i\right)D_{i,j} + \left(V - \overline{y}_j\right)E_{i,j}]B_{i,m}(u)B_{j,n}(v), \quad (4)$$

where $\overline{x}_i$ and $\overline{y}_j$ represent equal interval sampling according to the value of m and n, when $m = n = 3$, then the value of set $\left\{\overline{x}_i, \overline{y}_j\right\}$ is $\overline{x}_0 = \overline{y}_0 = 0$, $\overline{x}_1 = \overline{y}_1 = 1/m$, $\overline{x}_2 = \overline{y}_2 = 2/m$; $\overline{x}_3 = \overline{y}_3 = 1$, where $\left\{U, V \,\middle|\, 0 \le U \le 1; 0 \le V \le 1\right\}$, the sampling precision about u and v is

according to the values of m and n, $u=(U-\bar{x}_0)/(\bar{x}_m-\bar{x}_0)$, $v=(V-\bar{y}_0)/(\bar{y}_n-\bar{y}_0)$. $D_{i,j}$ is the x-directional derivative of point $p_{i,j}$, $E_{i,j}$ is the y-directional derivative of point $p_{i,j}$.

$$D_{ij}=\begin{cases}\dfrac{\alpha_{i,j}}{h_{i-1}+h_i}\left[h_i\dfrac{p_{i,j}-p_{i-1,j}}{h_{i-1}}+h_{i-1}\dfrac{p_{i+1,j}-p_{i,j}}{h_i}\right] & i\neq 0,\ m\\ \alpha_{0,j}\dfrac{p_{1,j}-p_{0,j}}{h_0} & i=0\\ \alpha_{m,j}\dfrac{p_{m,j}-p_{m-1,j}}{h_{m-1}} & i=m\end{cases},$$

$$E_{i,j}=\begin{cases}\dfrac{\beta_{i,j}}{f_{j-1}+k_j}\left[f_j\dfrac{p_{i,j}-p_{i,j-1}}{f_{j-1}}+f_{j-1}\dfrac{p_{i,j+1}-p_{i,j}}{f_j}\right] & j\neq 0,\ m\\ \beta_{i,0}\dfrac{p_{i,1}-p_{i,0}}{f_0} & j=0\\ \beta_{i,n}\dfrac{p_{i,n}-p_{i,n-1}}{f_{n-1}} & j=m\end{cases}, \tag{5}$$

here $f_j=\bar{y}_{j+1}-\bar{y}_j,(j=0,1,...,n-1)$ and $h_i=\bar{x}_{i+1}-\bar{x}_i$, $(i=0,1,...,m-1)$. $\alpha_{i,j}$ and $\beta_{i,j}$ are the shape parameters, and their values range is $[0,1]$. In our algorithm their assignment values are 0.8. Patch meshes generated by tensor-product Bezier are superior to the meshes of traditional method as a representation of genuine leaf surfaces, since they are much more compact, easier to manipulate, more closer to the original shape and have much better continuity properties.

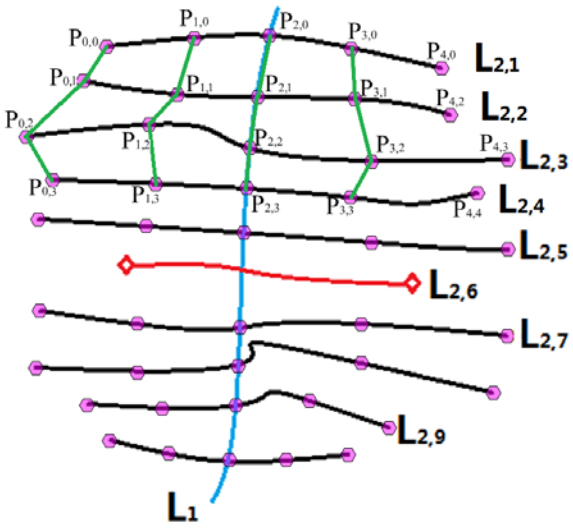

Fig. 3 Bicubic tensor-product Bezier surface algorithm implementation

Fig. 3 shows our tensor-product Bezier surface patches with degree $m\times n$, $m=3$, $n=3$. Note that control points $p_{i,j}$ of $(m+1)\times(n+1)$ number are organized topologically into m + 1 "rows" and n + 1 "column", where $i=1, 2, ..., m+1$, $j=1, 2, ..., n+1$. The control

points with skeleton lines and green lines in Fig. 3 composed control grid or control mesh of leaf surface. The control points for a bicubic patch are organized as follow matrix:

$$\begin{bmatrix} p_{0,0}, p_{1,0}, p_{2,0}, p_{3,0} \\ p_{0,1}, p_{1,1}, p_{2,1}, p_{3,1} \\ p_{0,2}, p_{1,2}, p_{2,2}, p_{3,2} \\ p_{0,3}, p_{1,3}, p_{2,3}, p_{3,3} \end{bmatrix},$$

then the bicubic tensor-product Bezier algorithm is applied to these points by turns, when all the points of foliage are calculated, the smoothing and unerring leaf surface Ω is constructed from TLS scanning data.

Leaves deformation under force

Leaves curling and growing are commonplace during the different season of the year, as they are part of most natural sceneries. Therefore modeling leaves is an important topic in computer graphics. Apart from possible static applications, it is usually important to have a time-varying representation of natural phenomena.

In this paper we focus on variety deformation of leaf types, such as sakura and michelia leave, the mesophyll construct the diverse leave surface, with an underlying venation that serves as both support to the leaf structure. The property of the mesophyll, together with the leaf venation, are the two factors that will most influence the leaf shape in our model. Combined with finite element method and dynamics driving deformation model, we create a tetrahedron 3D-mesh representation of the leaf surface and establish the mechanical field functions of foliage surface. When the external force is exerted on the leaves, stress intensity factor of each leave tetrahedron are analyzed and the offset of each tetrahedron vertex caused by external force are calculated.

Stress and strain analysis of leaves

Leaves are usually pliable, so small stresses applied over long times can result in ductile behavior. The stress or strain theory can characterizes their deformation, let $\Omega \subset R^3$ represents un-deformed or initial configuration of unerring leaf surface. $p\left(p_x, p_y, p_z\right) \in \Omega$ is one point on the leaf. After deformation, the deformed configuration of leaf is $\Omega' \subset R^3$, then there is a relative displacement $\boldsymbol{u}$ between every point on the leaf surface, denoted as: $p' = p + \boldsymbol{u}(p)$, where $p'\left(p'_x, p'_y, p'_z\right) \in \Omega'$. Supposing that $p_1, p_2 \in \Omega$ and $p'_1, p'_2 \in \Omega'$. The vector joining the position of point p_1 and p_2 is denoted as: $d = p_2 - p_1$, the same vector between p'_1 position and p'_2 position is denoted as: $d' = p'_2 - p'_1$, thus the relationship between $\boldsymbol{u}$ and $\boldsymbol{u}'$ is given by:

$$d' = p_2 + \boldsymbol{u}(p_2) - p_1 - \boldsymbol{u}(p_1) = d + \boldsymbol{u}(p_1 + d) - \boldsymbol{u}(p_1) = (I + \nabla \boldsymbol{u})d,$$

where I is the identity matrix, $I + \nabla \boldsymbol{u}$ is leaf deformation gradient tensor, which denoted as:

$$F = I + \nabla \boldsymbol{u},\ \nabla \boldsymbol{u} = \begin{bmatrix} \frac{\partial u}{\partial x} & \frac{\partial u}{\partial y} & \frac{\partial u}{\partial z} \\ \frac{\partial v}{\partial x} & \frac{\partial v}{\partial y} & \frac{\partial v}{\partial z} \\ \frac{\partial w}{\partial x} & \frac{\partial w}{\partial y} & \frac{\partial w}{\partial z} \end{bmatrix}. \tag{6}$$

The leaf deformation can represent as the transformation between d and d', just as:

$$\left|d'\right|^2 - \left|d\right|^2 = d'^{\mathrm{T}} d' - d^{\mathrm{T}} d = d^{\mathrm{T}} (F^{\mathrm{T}} F - I) d\,. \tag{7}$$

Combined with the elastic mechanics theorem and Eq. (7), the Green strain $E \in R^{3\times 3}$ is deduced as:

$$E = \frac{1}{2}(F^T F - I) = \frac{1}{2}(\nabla \boldsymbol{u} + \nabla \boldsymbol{u}^T + \nabla \boldsymbol{u}^T \nabla \boldsymbol{u})\,, \tag{8}$$

where E is an symmetric matrix. We consequently divide the leaf surface into a lot of tetrahedrons to calculate the movement distance of each tetrahedron vertex under stress or strain, so we can realize the simulation of deformed leaf. The four vertexes of each tetrahedron are denote as $t_i(x_i, y_i, z_i)$, $t_j(x_j, y_j, z_j)$, $t_k(x_k, y_k, z_k)$, $t_l(x_l, y_l, z_l)$. Each vertex has three degrees of freedom in the direction of X, Y and Z. After deformation, the displacement vector of each vertex is given by $\boldsymbol{u} = (u, v, w)^{\mathrm{T}}$, and the displacement functions of these vertexes can be expressed as a system of polynomial equations:

$$\begin{cases} u = C_{11} + C_{12} p_x + C_{13} p_y + C_{14} p_z \\ v = C_{21} + C_{22} p_x + C_{23} p_y + C_{34} p_z \\ w = C_{31} + C_{32} p_x + C_{33} p_y + C_{34} p_z \end{cases}. \tag{9}$$

Combining with the Eq. (9), deformation field functions are defined as:

$$\begin{cases} S_i = \frac{1}{6V}(a_i + b_i p_x + c_i p_y + d_i p_z) \\ S_j = \frac{1}{6V}(a_j + b_j p_x + c_j p_y + d_j p_z) \\ S_k = \frac{1}{6V}(a_k + b_k p_x + c_k p_y + d_k p_z) \\ S_l = \frac{1}{6V}(a_l + b_l p_x + c_l p_y + d_l p_z) \end{cases}, \tag{10}$$

where S_i is the interpolation function about each vertex, V is the tetrahedral volume,

$$V=\frac{1}{6}\begin{vmatrix}1 & x_i & y_i & z_i\\ 1 & x_j & y_j & z_j\\ 1 & x_k & y_k & z_k\\ 1 & x_l & y_l & z_l\end{vmatrix}, \text{ and}$$

$$a_i=\begin{vmatrix}x_j & y_j & z_j\\ x_k & y_k & z_k\\ x_l & y_l & z_l\end{vmatrix},\ b_i=-\begin{vmatrix}1 & y_j & z_j\\ 1 & y_k & z_k\\ 1 & y_l & z_l\end{vmatrix},\ c_i=\begin{vmatrix}x_j & 1 & z_j\\ x_k & 1 & z_k\\ x_l & 1 & z_l\end{vmatrix},\ d_i=-\begin{vmatrix}x_j & y_j & 1\\ x_k & y_k & 1\\ x_l & y_l & 1\end{vmatrix}.$$

For the variables of a_j, b_j, c_j, d_j, ..., a_k, ..., a_l, b_l, c_l, d_l, we can use right hand rule to change the subscript of x, y, z according to the order of i, j, k, l. For example

$$a_j=\begin{vmatrix}x_k & y_k & z_k\\ x_l & y_l & z_l\\ x_i & y_i & z_i\end{vmatrix},\ a_k=\begin{vmatrix}x_l & y_l & z_l\\ x_i & y_i & z_i\\ x_j & y_j & z_j\end{vmatrix},\ a_l=\begin{vmatrix}x_i & y_i & z_i\\ x_j & y_j & z_j\\ x_k & y_k & z_k\end{vmatrix},$$

and the displacement vector has the form:

$$\boldsymbol{u}=\begin{bmatrix}u\\ v\\ w\end{bmatrix}=[IS_i\ \ IS_j\ \ IS_k\ \ IS_l]\begin{bmatrix}\vec{t}_i\\ \vec{t}_j\\ \vec{t}_k\\ \vec{t}_l\end{bmatrix}, \tag{11}$$

where $\left[\vec{t}_i\ \vec{t}_j\ \vec{t}_k\ \vec{t}_l\right]^{\mathrm{T}}$ is displacement vector of each tetrahedron vertex, I is identity matrix, every column vector of matrix $\boldsymbol{u}$ is the displacement tensor of each vertex, thus second-order Piola-Kirchhoff tensor σ is calculated, which is a 3×3 symmetric matrix, just as:

$$\boldsymbol{\sigma}=\begin{bmatrix}\sigma_{xx} & \sigma_{xy} & \sigma_{xz}\\ \sigma_{yx} & \sigma_{yy} & \sigma_{yz}\\ \sigma_{zx} & \sigma_{zy} & \sigma_{zz}\end{bmatrix}=\begin{bmatrix}u_x & \left(u_y+v_x\right)/2 & \left(u_z+w_x\right)/2\\ \left(u_y+v_x\right)/2 & v_y & \left(v_z+w_y\right)/2\\ \left(u_z+w_x\right)/2 & \left(v_z+w_y\right)/2 & w_z\end{bmatrix}. \tag{12}$$

Leaf material definition and motion control

We apply a linear isotropic elastic material to represent the leaf model. In order to define the biological properties of leaves, we set two parameters, such as: Young modulus Y and Poisson ratio V, analogously, Lame constant μ and λ, or bulk modulus K and shear modulus G. The group of two parameters can represent leaf properties enough, and these parameters are equivalent and interchangeable. The transformation between them is shown in Table 2. For example, if we have got the values of Y and V, other parameters can be calculated based on the function φ_1, just as:

$$K=\frac{Y}{3(1-2V)},\ G=\frac{Y}{3(1+V)},\ \lambda=\frac{YV}{(1+V)(1-2V)},\ \mu=\frac{Y}{2(1+V)}.$$

Table 2. The transformation between various materials properties

Material properties	Young modulus Y	Poisson ratio V	Bulk modulus K	Shear modulus G	Lame constant λ	Lame constant μ
$\varphi_1(E,v)$			$\frac{Y}{3(1-2V)}$	$\frac{Y}{3(1+V)}$	$\frac{YV}{(1+V)(1-2V)}$	$\frac{Y}{2(1+V)}$
$\varphi_2(K,G)$	$\frac{9KG}{3K+G}$	$\frac{1}{2}\left(1-\frac{3G}{3K+G}\right)$			$K-\frac{2G}{3}$	G
$\varphi_3(\lambda,\mu)$	$\mu\frac{3\lambda+2\mu}{\lambda+\mu}$	$\frac{\lambda}{2(\lambda+\mu)}$	$\lambda+\frac{2\mu}{3}$	μ		

In order to simulate the leaf motivation, we consequently adopt Venant-Kirchhoff model [1] which is defined by a linear stress-strain relationship of the form:

$$\zeta = \lambda\left(tr\left(E\right)\right)I_3 + 2\mu E, \tag{13}$$

where ζ is the second Piola stress tensor, E is the Green-Lagrange strain tensor, I_3 is the 3×3 identity matrix, λ and μ are (possibly spatially varying) Lame constants. It is an example of a hyper-elastic isotropic material: elastic strain energy is a unique function of leaf deformation only (and not of deformation history), and at any location, material is equally stretchable in all directions. Then, by the finite element method and discretization ideal, the leaf is transformed to tetrahedron meshes, the motion of a deformable leaf can be described by the Euler-Lagrange equation, which is a second order system of ordinary differential equations:

$$M\ddot{\boldsymbol{u}} + D\dot{\boldsymbol{u}} + R(\boldsymbol{u}) = f_{ext}. \tag{14}$$

Here, $\boldsymbol{u} \in R^{3n}$ is the displacement vector (the unknown), $M \in R^{3n,3n}$ is the mass matrix, $D \in R^{3n,3n}$ are damping forces, and $R(\boldsymbol{u})$ are internal deformation forces. The mass matrix depends only on the leaf's mesh and mass density distribution. Internal forces corresponding to the displacement $\boldsymbol{u}$ are given by the vector $R(\boldsymbol{u}) \in R^3$. The mapping R is nonlinear due to the nonlinearity of the Green-Lagrange strain tensor, and (in general) due to any material nonlinearities. Note that the matrix M, and the mappings D and R are independent of time. Apart from $\boldsymbol{u}$, the only time-dependent term in the equation is the vector of external forces f_{ext}, used to model. Let $K\left(\boldsymbol{u}\right) \in R^{3n,3n}$ denote the Jacobian matrix of the internal forces R, it is the tangent stiffness matrix. Then, we use a local Rayleigh damping model of the form:

$$D = \left(\alpha M + \beta K\right)\dot{\boldsymbol{u}}. \tag{15}$$

This damping model is controlled by two positive real-valued parameters, α and β, which roughly have the effect of damping low and high time-frequency components of deformations respectively.

The solutions of our algorithm

Due to high deviation and big dispersion of the leaf PCD, so we adopt Pro/Enginee software to realize the conversion between the discrete points to leaf 3D surface. Firstly the midvein is

properly added into the leaf surface, and leaf veins and mesophyll are assigned to different material properties. Secondly, combing with COMSOL multi-physics processing software, the leaf model is divided into many tetrahedrons with proper mesh size. Finally, by applying an external force on leaf model, the displacement of every tetrahedral are obtained from the solution of our deformation equations, and three-dimension deformation of a leaf is generated by the controllability grid bending.

Results and discussion

In this study, a TLS of Leica Scan Station C10 was used for data collection and leaf structure measurement about individual michelia tree and sakura tree on campus. The michelia leaf is larger with density PCD, so it is easier to construct its leaf surface, however, the sakura leaf is smaller with relatively sparse data with noise and interference existing among leaf PCD, but our proposed algorithm can effectively construct different sakura leaf model and delineate the varying deformed leaf morphology under different external force. The specific results are shown as below.

Experiment of leaf model construction

The experimental results of our method are shown in Fig. 4 (a1)-(h1) demonstrate modeling process of Michelia leaves, and (a2)-(h2) illustrate modeling process of sakura tree leaves. (a) is the scanned leaf PCD; (c)(d) use our polynomial fitting and surface intersection algorithm to locate the real foliage boundary. After generalized bicubic Bezier surface fitting process, (e)(f) show the smooth leaf PCD in red. (g)(h) are the foliar reconstruction 3D model by our method, which is composed of mesophyll and vein with different material properties, and we list material property values of different leaf parts in Table 3.

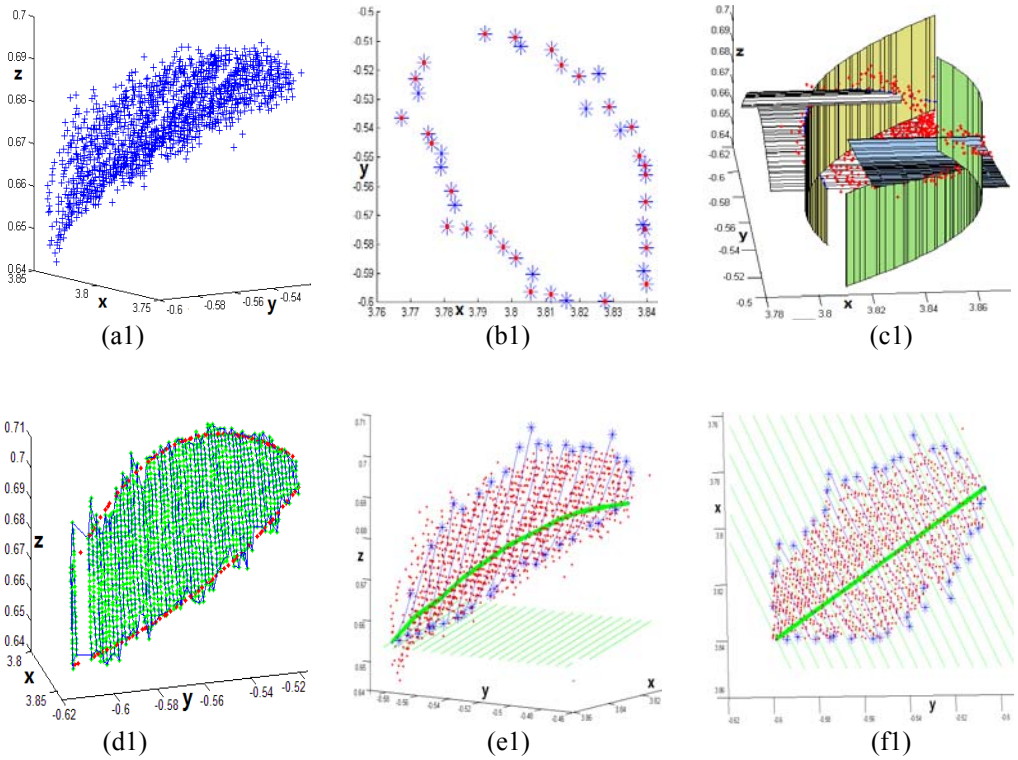

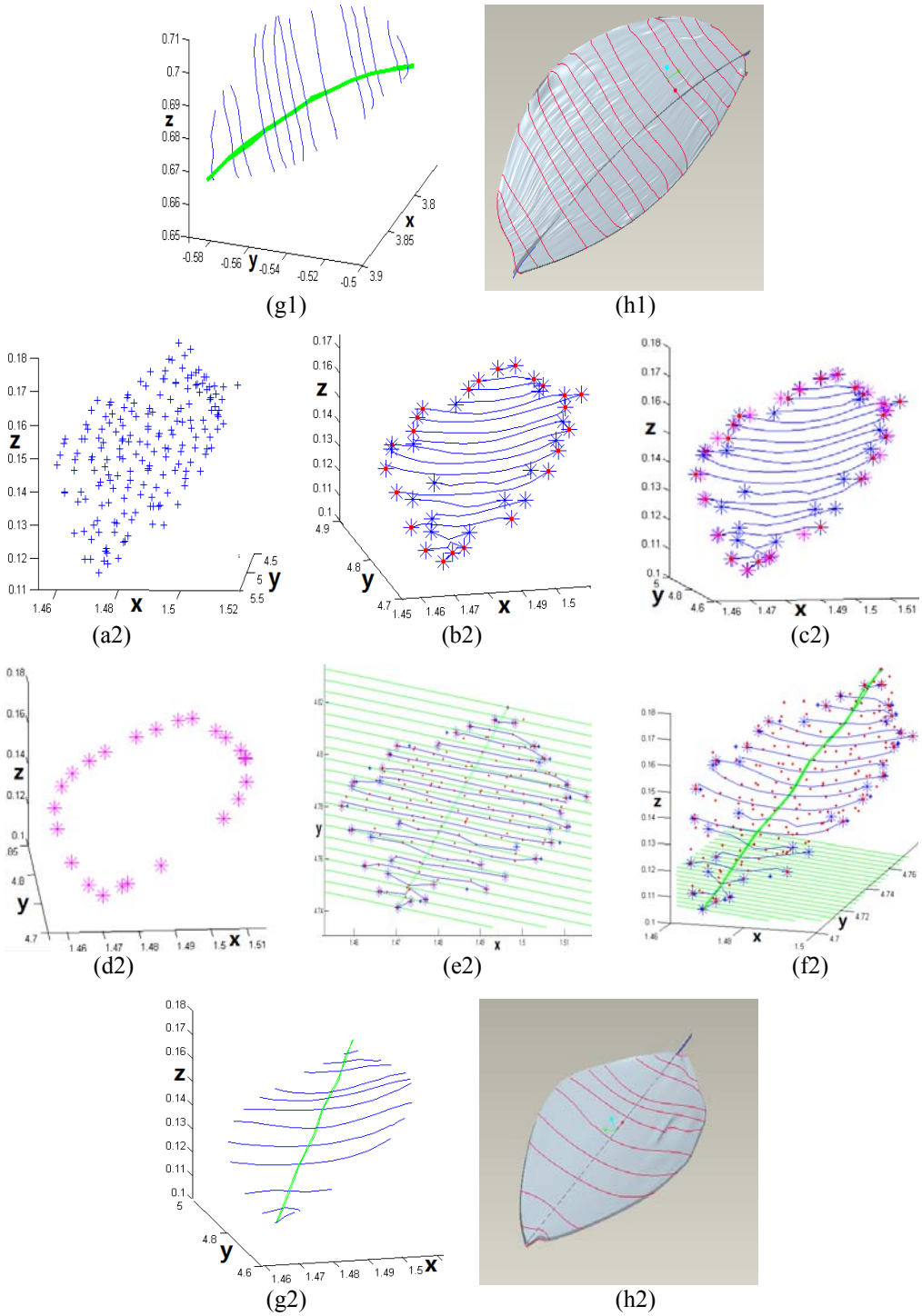

Fig. 4 Foliage 3D reconstruction of our method

Table 3. The material properties of leaf models used in our paper

	Mesophyll of michelia leaf	**Vein of michelia leaf**	**Mesophyll of sakura leaf**	**Vein of sakura leaf**
Density, (kg/m^3)	0.32	0.75	0.28	0.69
Young's modulus, (Pa)	0.04	0.19	0.03	0.11
Poisson ratio	0.73	0.54	0.82	0.69

Experiment of leaf deformation under external force

Fig. 5 demonstrates the deformation under external force, experimental subject of (1) is Michelia leaf, and experimental subject of (2) is sakura leaf. (a) (b) illustrate the mesophyll and vein of leaf model subdivided by tetrahedron. When external force act on the triangle mesh, deformed leaves are demonstrated in (c) (d) (e) (f). If we fix top petiole of the leaf, and applying different tensile force at the other end of the midvein, the deformed leaf is shown in (c) (d). If we keep the whole midvein fixed and exert a pulling force on leaf both edge, the deformed results are demonstrated in (e) (f). Specific experimental parameters are shown in Table 4. According to the experimental results shown in Fig. 5, we believe our method is versatile enough to be applied in a much larger variety of plant leaves under different external force than the few presented here.

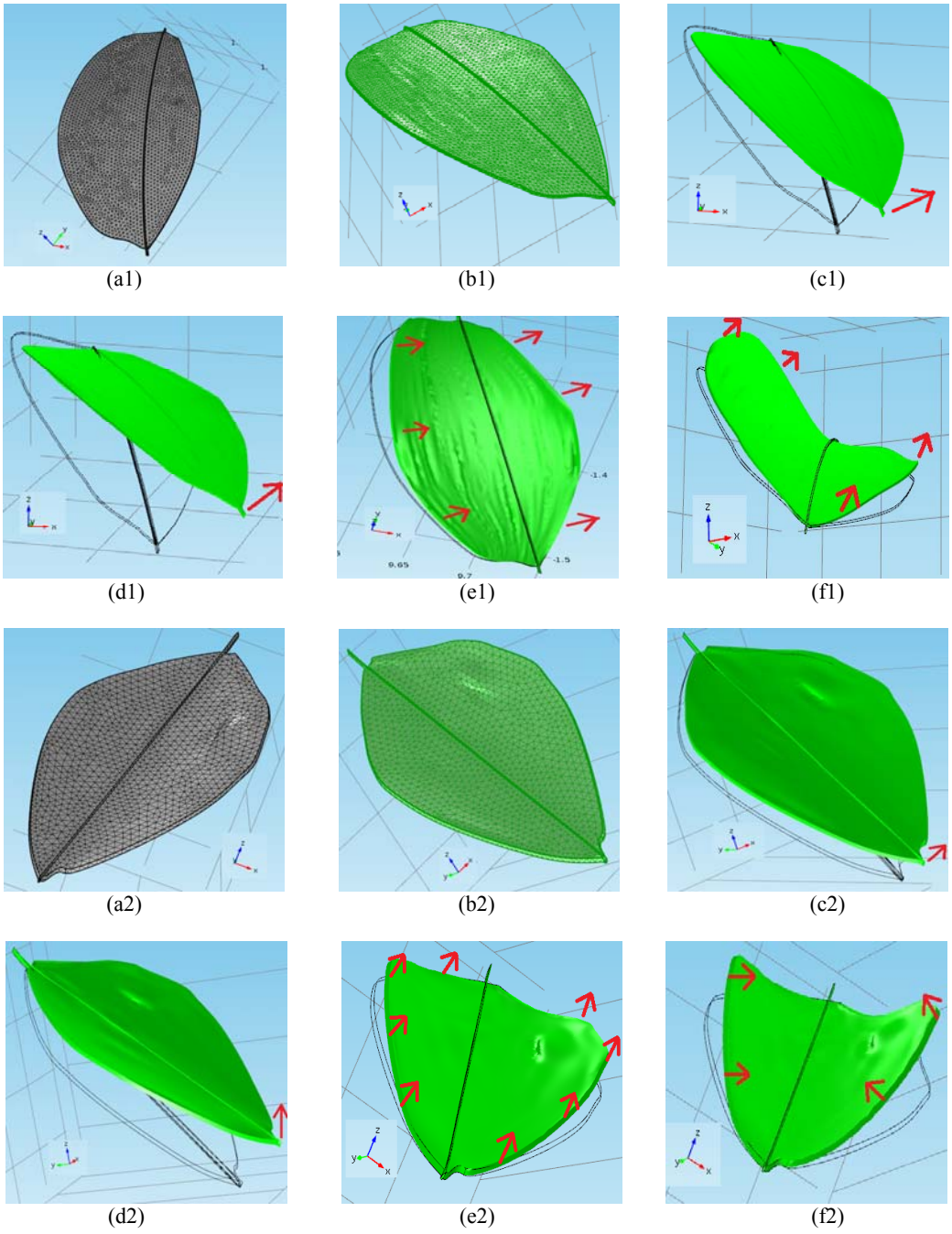

Fig. 5 Leaf surface meshing and deformation under force

Table 4. The material properties of leaf models used in our paper

	Number of the constructed tetrahedron	Initial leaf area, (cm^2)	Deformed leaf area, (cm^2)
Michelia leaf	Mesophyll 3212 Vein 487	63.03	65.13
Sakura leaf	Mesophyll 879 Vein 148	15.72	16.93

Conclusion

In this paper, we present a method for leaf 3D reconstruction and deformation. Firstly, we use Leica C10 laser scanner to obtain the PCD of Michelia and sakura leaf on campus, and combing with the polynomial fitting method and algorithm of generalized bicubic tensor product Bezier, real leaf boundary and smooth leaf model are calculated without noise existing. Secondly, the leaf model is divided into two parts, mesophyll and vein with different material properties. Combing with finite element decomposition method and mechanical analysis function, the detailed deformation pattern of the leaf can be simulated under various external forces. Finally, taking the michelia and sakura leaves as the experimental sample, our proposed method is proved effective and robust. In the following work, we will study the natural plant tissue deformation in growing or senescence processes via the application of membrane gel swelling or deswelling and hence the fantasying phenomena of nature may be scientifically explained.

Acknowledgements

This work is supported by National Natural Science Foundation of China (31300472), Natural Science Foundation of Jiangsu Province (BK2012418, BK2012815), High Academic Qualifications Fund of Nanjing Forestry University (163070052, 163070036), Project Funded by the Priority Academic Program Development of Jiangsu Higher Education Institutions. Moreover, we appreciate the advanced analysis and testing center of Nanjing Forestry University that provide the Leica TLS apparatus for our experimental data collection.

References

1. Capell S., S. Green, B. Curless, T. Duchamp (2002). Interactive Skeleton-driven Dynamic Deformations, ACM Transactions on Graphics, 21(3), 586-593.
2. Chi X. Y., B. Sheng, Y. Y. Chen, E. H. Wu (2009). Physically Based Simulation of Weathering Plant Leaves, Chinese Journal of Computers, 32(2), 221-230.
3. Liu Z. S., W. Hong, Z. G. Suo (2010). Modeling and Simulation of Buckling of Polymeric Membrane Thin Film Gel, Computational Materials Science, 49(1) Supplement, S60-S64.
4. Lovell J. L., D. L. B. Jupp, G. J. Newnhamc (2011). Measuring Tree Stem Diameters using Intensity Profiles from Ground-based Scanning Lidar from a Fixed Viewpoint, ISPRS Journal of Photogrammetry and Remote Sensing, 66, 46-55.
5. Seidela D., S. Fleckb, C. Leuschner (2012). Analyzing Forest Canopies with Ground-based Laser Scanning: A Comparison with Hemispherical Photography, Agricultural and Forest Meteorology, 154, 1-8.
6. Xu H., N. Gossett, B. Q. Chen (2007). Knowledge and Heuristic Based Modeling of Laser-scanned Trees, ACM Transactions on Graphics, 26, 1-19.

7. Zeng L. Q., Q. W. Han, H. C. Qu, Z. H. Lu (2010). Leaf Muti-scale Variation Algorithm under Functional Structural Plant Model, Journal of Computational Information Systems, 6(5), 1449-1457.
8. Zheng G., M. L. Moskal (2012). Computational-geometry-based Retrieval of Effective Leaf Area Index Using Terrestrial Laser Scanning, IEEE Transactions on Geoscience Electronics, 50, 3958-3969.
9. Zheng G., M. L. Moskal (2012). Leaf Orientation Retrieval from Terrestrial Laser Scanning (TLS) Data, IEEE Transactions on Geoscience and Remote Sensing, 50, 3970-3979.
10. Zhu C., W. L. Meng, Y. H. Wang, X. P. Zhang (2011). Cage-based Tree Deformation, Lecture Notes in Computer Science, 6872, 409-413.

Assoc. Prof. Ting Yun, Ph.D.
E-mail: njyunting@qq.com

Ting Yun received his Ph.D. (2008) from Nanjing University of Science and Technology, China. Now he is an Associate Professor of department of information science and technology, Nanjing Forestry University. His research interests includes: woodland survey, computational biology, computer graphics and image processing.

Weizheng Li, Ph.D.
E-mail: gisplayer@gmail.com

Weizheng Li received his Ph.D. (2009) from Nanjing Forestry University, China. Now he is a Senior laboratory technician of Advanced Analysis and Testing Center, Nanjing Forestry University. His research interests includes: geographical information system, analysis of laser point cloud data, woodland measurement by airborne lidar.

Assoc. Prof. Yuan Sun, Ph.D.
E-mail: sunyuan1123@126.com

Yuan Sun received her Ph.D. (2011) from University of Freiburg, Germany. Now he is an Associate professor of Department of Forest Resource and Environment, Nanjing Forestry University, China. Her research interests includes: woodland survey, forest management, dendrology.

Assoc. Prof. Lianfeng Xue, Ph.D.
E-mail: 285201972@qq.com

Lianfeng Xue received her Ph.D. (2012) from Nanjing Forestry University, China. Now she is an Associate professor of Department of Information Science and Technology, Nanjing Forestry University. Her research interests includes: virtual reality, biomedical signal processing, computer simulation.